Toxicology Research

Accepted Manuscript

ROYAL SOCIETY OF CHEMISTRY

www.rsc.org/toxicology

Sodium tanshinone IIA sulfonate suppresses pulmonary fibroblast proliferation and activation induced by silica: role of the Nrf2/Trx pathway

Zhonghui Zhu 1,2, Yan Wang 1,2, Di Liang 1,2,Gengxia Yang 3, Li Chen 1,2, Piye Niu 1,2, Lin Tian 1,2*

1School of Public Health, Capital Medical University, Beijing 100069, China

2Beijing Key Laboratory of Environmental Toxicology, Capital Medical University, Beijing, 100069, P.R. China

3Oncology Minimally Invasive Interventional Center, Beijing Youan Hospital, Capital Medical University, Beijing 100069, China

*Corresponding author: Lin Tian, M.D., Ph.D.

Department of Occupational Health and Environmental Health, School of Public Health, Capital Medical University, Beijing 100069, China.

Tel.: +86 10 83911506; fax: +86 10 83911506.

E-mail address: tian_lin@163.com

Abstract

Alveolar macrophages are believed to induce oxidative stress via reactive oxygen species (ROS) when silica particles are inhaled. This process can contribute to the pathogenesis of silicosis, but the mechanism is unclear. A traditional Chinese herbal derivative, sodium tanshinone IIA sulfonate (STS), displays significant antioxidant effects. Here, we determine whether STS can attenuate the oxidative stress induced by silica. Traditionally, studies on the toxic effects of silica have focused on monocultures of macrophages or fibroblasts. A coculture model of macrophages (Raw 264.7) and pulmonary fibroblasts (MRC-5) was used in this study to mimic a more *in vivo*-like environment. We investigated the protective effects of STS on the abnormal proliferation of MRC-5 fibroblasts in an *in vitro* model. The results showed that fibroblast viability increased with the accumulation of intracellular ROS induced by cocultured Raw 264.7 cells after silica exposure. Treatment with STS markedly ameliorated the silica-induced cell proliferation and oxidative stress. Western blotting and immunofluorescence analysis of the Nrf2 and thioredoxin (Trx) system were conducted, and the results confirmed that treatment with STS enhanced nuclear Nrf2 accumulation and mediated antioxidant Trx system expression. These findings suggest that silica exposure might induce some level of oxidative stress in fibroblasts and that STS might augment antioxidant activities via up-regulation of the Nrf2 and Trx system pathways in MRC-5 cells *in vitro*.

Keywords

Silicosis; Sodium tanshinone IIA sulfonate; Fibroblast; ROS;Nrf2;Trx

1. Introduction

Silicosis, a disease caused by chronic inhalation of crystalline silica, is characterized by inflammation and scarring in the form of nodular lesions in the lungs. The presence of silicosis has been known for centuries, and industrial dust has led to the increase of silicosis worldwide, especially in developing countries. However, the pathological mechanism of silicosis is unclear. Recent studies have found that when silica particle is inhaled, it is inevitably engulfed by macrophages that act as the primary barrier and release cytokines, such as TGF-β1 (1). These stimulate fibroblast proliferation and the production of collagen around the silica particles, resulting in pulmonary fibrosis and the formation of silicotic nodules (2). However, enhancing anti-inflammatory therapy has shown limited therapeutic efficacy in silicosis.

During the development of silicosis, contact between alveolar macrophages and silica drives the subsequent pathogenic process. The uptake of silica particles by macrophages triggers the production of reactive oxygen species (ROS) via the oxidative stress pathway, which in turn contributes to pulmonary damage and macrophage death by apoptosis (3). In addition, recent evidence has suggested that nonphagocytic cells, including fibroblasts, also produce ROS following stimulation by cytokines and growth factors (4) (5). Sustained ROS generation perpetuates the continuum of phagocytosis, cell death, inflammatory cell recruitment and silica deposition, and it is responsible for progressive and irreversible lung injury (6) (7) (8). These data suggest that scavenging excessive ROS could be a possible therapeutic approach to modulate the fibrogenic response.

Over the past few decades, studies have found an emerging role for the transcription factor nuclear factor (erythroid-derived 2)-like 2 (Nrf2) in resistance to oxidative stress. Under normal conditions, Nrf2 is predominantly sequestered in the cytoplasm with its chaperone. Oxidative insults cause dissociation of the chaperone complex, triggering the translocation of Nrf2 from the cytoplasm to the nucleus (9). Then, nuclear Nrf2 binds to the antioxidant response element (ARE) and up-regulates the transcription of genes, such as thioredoxin (Trx) and thioredoxin reductase (TrxR)

(10), which are critical to the cellular antioxidant process (11) (12). Trx, TrxR and NADPH comprise the Trx system, which plays an important role in some biological functions such as the regulation of redox (13). To clear ROS, TrxR is involved in catalyzing oxidized Trx to regenerate its reduced form using NADPH (14). We have previously observed the relationship between Nrf2 and Trx in a rat silicosis model (15). In addition, knockdown of Nrf2 in mice can substantially increase susceptibility to a variety of exogenous toxicities and disease situations associated with oxidative pathology (16) (17) (18), whereas pharmacological boosting of Nrf2 activity with chemoprotective agents protects animals from oxidative damage (19). However, activating the Nrf2 and Trx pathways has seldom been studied in alleviating oxidative stress in silicosis.

Sodium tanshinone IIA sulfonate (STS) is a water-soluble derivative of tanshinone IIA, an important ingredient in the well-known traditional Chinese herb Danshen (Salvia miltiorrhiza). With superior bio-availability and various pharmacological actions, STS has been used for the treatment of antioxidative stress and reversing myocardial fibrosis, among other conditions (20). However, there are few studies available on the efficacy of STS in pulmonary fibrosis, and the exact mechanisms of the protective actions of STS in silicosis remain largely undefinable.

Monoculture studies of pulmonary fibroblasts are the predominant form of silica particle toxicological testing *in vitro*, but it is difficult to show the specific mechanism of silica particle pathogenesis both *in vitro* and *in vivo*. Cocultures of multiple cell types have been proposed to be superior to monoculture and to more adequately reflect a signaling environment *in vivo* (21) (22). In this study, we cocultured macrophages (Raw 264.7) with lung fibroblasts (MRC-5) in a transwell system to determine the potential toxic effects of silica particles and to explore the protective effects of STS. The effects were indirectly similar to those observed in lung tissue and further support the hypothesis that macrophages mediate the pulmonary response following silica exposure. Through the measurement of crystalline silica particles, ROS production, fibroblast viability, and transcription factor and downstream antioxidant protein expression in MRC-5, this study determined that silica exposure

may induce oxidative stress to stimulate the proliferation of fibroblasts and that treatment with STS may augment antioxidant activities via the up-regulation of Nrf2/Trx to restore the oxidant/antioxidant equilibrium and to attenuate MRC-5 fibroblast activation *in vitro*.

2. Materials and methods

2.1 Silica particles and STS

Silica particles (Sigma-Aldrich Co. LLC.) with a nominal size of 0.5-10 μm (approx. 80% between 1-5 μm) were used. The morphology of the crystalline silica particles was assessed by transmission electron microscopy (TEM, JEOL, JEM-2100) and scanning electron microscopy (SEM, HITACHI, S-4800) (Fig. 1A&B). For cell culture, silica was first prepared as stock solution in phosphate-buffered saline (PBS) at a final concentration of 2 mg/mL after sonication. The silica stock solution was kept at 4°C and used within 1 week.

STS was obtained from the National Institutes for Food and Drug Control (Beijing, China) and was prepared fresh as a 0.5 mg/mL stock solution in PBS. The molecule structure of STS is shown in Fig. 1C.

2.2 Cell culture

Human fetal lung fibroblasts (MRC-5) (Cell Culture Center of Peking Union Medical College, China) and murine macrophage cells (Raw 264.7) (Xiang Ya Central Experiment Laboratory, China) were used in this experiment. Briefly, MRC-5 cells were cultured in minimal essential medium (MEM) with 10% fetal bovine serum (FBS, Gibco) and 1% non-essential amino acids (NEAA, Gibco). Raw 264.7 cells were grown in Dulbecco's modified Eagle's medium (DMEM) and supplemented with 10% FBS, 100 units/mL penicillin G (Sigma), and 100 mg/mL streptomycin (Sigma). All cells were maintained in an incubator at 37°C and 5% CO_2.

To prepare the coculture, inserts with a 0.4 μm pore size were removed from a polyester Transwell (Corning, USA) and seeded with Raw 264.7 cells (6-well Transwell: 1.5×10^5 cells/well, 96-well Transwell: 3×10^3 cells/well, individually) in complete media in an empty companion dish for at least 12 h. MRC-5 cells (6-well Transwell: 2×10^5 cells/well, 96-well Transwell: 4×10^3 cells/well, individually) were

plated at the bottom of each plate well and allowed to adhere for at least 12 h without apical chamber inserts. Then, the inserts were returned to the Transwell. MRC-5 cells were maintained in 2.5 ml or 235 µl of MEM without serum in the basolateral chamber while Raw 264.7 cells were maintained in 1.5 ml or 75 µl of DMEM without serum in the apical chamber. Cells were exposed to silica solution at a final concentration of 12.5, 25, 50, or 100 µg/mL for 24 h. As the control group, an MRC-5 monoculture was seeded on the Transwell, and as the negative control group, a coculture of Raw 264.7 and MRC-5 cells without silica was kept under the same culture conditions. Furthermore, to explore the role of STS, MRC-5 cells were supplemented with various concentrations of STS (0, 1, 5, 10, 25, or 50 µg/mL) in the basolateral chamber with silica exposure (final concentration of 50 µg/mL only) and co-incubated for 24 h (Fig. 1D).

2.3 Cell viability

The measurement of cell viability was performed using an MTT ((4, 5-dimethylthiazol-2-yl)-2, 5-diphenyl tetrazolium bromide) assay. Briefly, Raw 264.7 cells were plated in the 96-well chamber inserts, and MRC-5 cells were added to the bottom; the cells were then incubated at 37°C for 12 h. As a control group, MRC-5 cells were solo seeded at 4×10^3 cells/well before incubating for 12 h. Then cells were treated with various concentrations of STS and/or silica suspension and then incubated at 37°C for an additional 24 h in silica/STS groups. Alternatively, the medium was replaced with DMEM containing a final concentration of 10^{-3}, 10^{-4}, 10^{-5}, 10^{-6}, or 10^{-7} M H_2O_2 and cultured for 24 h. After the incubation, the inserts and media in the bottom were removed, and then, 100 µL of MTT solution (0.5 mg/mL in PBS) and 100 µL of DMEM were added into each bottom well. MRC-5 cells were incubated under the same conditions for an additional 4 h. MTT was cleaved by living cells into visible formazan crystals during this incubation. The formazan crystals were dissolved in DMSO, and the resulting absorbance was measured at 490 nm using an enzyme-linked immunosorbent assay. The relative cell viability was calculated and compared with the absorbance of the negative control group. All MTT assays were performed more than five times.

2.4 Intracellular ROS measurement

Intracellular ROS production was analyzed using a DCFH-DA probe according to the manufacturer's instructions (Jiancheng Biotech, Nanjing, China). DCFH-DA, a nonfluorescent cell-permeant compound, is cleaved by endogenous esterases within the cell, and the de-esterified product can be converted into the fluorescent compound DCF upon oxidation by intracellular ROS. To estimate intracellular ROS, after 24 h of incubation, MRC-5 cells were loaded with 100 nM DCFH-DA for 10 minutes at 37°C, washed with PBS, and immediately analyzed using a fluorospectrophotometer (SHIMADZU, RF-5301PC) at an excitation wavelength of 485 nm and an emission wavelength of 538 nm. The level of total ROS is expressed as fluorescence intensity/mg protein.

2.5 Western blot analysis

Whole MRC-5 extracts were prepared using lysis buffer (50 mM Tris ·HCl, pH 7.4; 150 mM NaCl; 1% sodium deoxycholate; 0.1% SDS) (KeyGEN Biotech, China) on ice after 24 h of incubation. The protein concentration was determined by Bicinchoninic acid (BCA) assay (Thermo Scientific, Rockford, IL, USA). Equal amounts of protein extracts (50 μg) were separated by 10% or 15% SDS-Polyacrylamide gel electrophoresis and then transferred onto a polyvinylidene difluoride (PVDF) membrane (GE Healthcare, Piscataway, NJ, USA). The transblotted membranes were blocked with 5% nonfat milk in TBS containing 0.1% Tween 20 (TBST) for 1 h. The membranes were incubated overnight at 4°C with specific antibodies against Nrf2 (1:1000 dilution, Abcam, UK), Trx (1:1000 dilution, Cell Signaling Technology, USA), TrxR (1:500 dilution, Santa Cruz Biotechnology, USA) and β-actin (1:1000 dilution, Cell Signaling Technology, USA). The blots were then incubated with the corresponding horseradish peroxidase (HRP)-conjugated secondary antibody (1:2000 dilution, Cell Signaling, USA) for 2 h. The blots were developed using ECL plus western blot detection reagents (Thermo Scientific, USA) and detected with a Molecular Imager Bio-Rad Gel Doc™ XR+ with Image Lab™ Software (Bio-Rad, California, USA).

2.6 Confocal laser scanning microscopy

Immunofluorescence labeling was performed to assess the subcellular localization of Nrf2 (1:200 dilution, Abcam, UK) and Trx (1:200 dilution, Abcam, UK) in MRC-5 cultures. Nuclear immunofluorescence was quantified by co-localization with DAPI under observation with a LEICA TCS SP8X (LEICA, Germany).

2.7 Knockdown of Nrf2 by lentiviral transfection

Nrf2-shRNAs were designed to target the Nrf2 gene (NM_001145412); the specific shRNA sequences were cloned into GV248 (Shanghai GeneChem Co., Ltd., Shanghai, China). A green fluorescent protein (GFP) lentiviral vector was used as a negative control. The lentivirus was produced by transfecting lentiviral plasmids into HEK-293T cells with Lipofectamine 2000 (Invitrogen). After transfection for 48 h, cell supernatant containing the lentivirus was harvested and concentrated, and the virus titer was calibrated. The lentivirus, with a final concentration of 4×10^8 TU/ml, was stored at $-80°C$.

MRC-5 cells were plated at a density of 1×10^4 cells/well in six-well plates in MEM supplemented with 10% FBS and 1% NEAA in a humidified atmosphere of 5% CO_2 at 37°C for 12 h before transfection. The medium was then replaced with 1 ml of serum-free medium, and the cells were transfected with lentivirus at a multiplicity of infection (MOI) of 10 in the presence of 5 μg/ml polybrene (Sigma). The medium was changed to complete medium after 12 h of transfection. After 72 h of incubation, the rate of infection was observed using a fluorescence microscope, and the total cellular RNA was extracted for further validation or the transfected cells were used for cell function experiments.

2.8 RNA isolation and reverse transcription–polymerase chain reaction

At the indicated time points, total RNA was isolated with the SV Total RNA Isolation System (Promega) and spectrophotometrically quantified, and reverse transcription–polymerase chain reaction (RT-PCR) was performed with the OneTaq® RT-PCR Kit (New England Biolabs) according to the manufacturer's instructions. The reactions were started at first-strand cDNA synthesis, with incubation at 42°C for one

hour. The PCR cycling conditions were as follows: 95°C for 30 seconds and then immediately cycled 30 times through a 30-second denaturing step at 94°C, a 30-second annealing step at 61°C, and a 1-min extension step at 68°C. After the cycling procedure, a final 5-min elongation step at 68°C was performed. All amplifications were performed in the linear range of the assay. The reaction products were separated on a 1.0% agarose gel and imaged using a Molecular Imager Bio-Rad Gel Doc^{TM} XR+ with Image Lab^{TM} Software (BIO-RAD, California, USA). The primers used are shown in table 1.

2.9 Statistical analysis

Individual dependent variable data were analyzed statistically by one-way analysis of variance (ANOVA), followed by Duncan's multiple range test when appropriate. Differences between groups were considered to be significant when $p<0.05$. Data are expressed as the mean ±S.D.

3. Results

3.1 Effect of STS on the suppression of both silica- and H_2O_2-induced MRC-5 proliferation.

We first explored the viability of MRC-5 cells following treatment with either silica or H_2O_2 by MTT assay. As shown in Fig. 2A, the viability of MRC-5 cells cocultured with Raw 264.7 cells was increased compared with the quiescent monocultured MRC-5 cells, while at low concentrations (12.5 or 25 μg/mL) silica administration had an impact on cocultured MRC-5 cells. When examining cells treated with higher amounts of silica, MRC-5 fibroblasts treated with 50 μg/mL silica showed peak and significant proliferation compared with the cocultured group without silica treatment. Based on this result, 50 μg/mL silica was used for all subsequent STS treatment experiments. As shown in Fig. 2B, a range of concentrations of H_2O_2 (10^{-3}, 10^{-4}, 10^{-5}, 10^{-6}, and 10^{-7} M) were used to determine their effects on MRC-5 cell proliferation. In the case of H_2O_2, an increase of $20 - 30\%$ in cell proliferation compared with the control group was measured after treatment with

10^{-5} M H_2O_2, which was the concentration that was determined for the subsequent study. As the concentration increased further to 10^{-4} M, the toxic effect of H_2O_2 became apparent. Furthermore, the toxicity of STS on MRC-5 was not obvious upto 10 μg/mL in Fig 2C. The effects of various STS concentrations below 10 μg/mL were measured following their addition after silica or H_2O_2 treatment as indication previously. As shown in Fig. 2D, STS treatment (10 μg/mL) suppressed the MRC-5 proliferation induced by 50 μg/mL silica. STS administration also showed similar effects on the cell proliferation induced by 10^{-5} M H_2O_2 (Fig. 2E).

3.2 Effect of STS on the inhibition of silica-induced MRC-5 activation.

To evaluate whether fibroblast activation plays a key role in silicosis, the expression of extracellular matrix proteins (collagen I and III) was determined. As shown in Fig. 3 A&B, corresponding with MRC-5 proliferation, both collagen I expression and collagen III expression were increased in a silica-concentration-dependent manner. The expression of collagen in the 50 μg/mL silica treatment groups was significantly increased compared to the negative control group. We also used different concentrations of STS to elucidate the possible effects of STS on extracellular matrix degradation. Compared to the silica treatment group, STS treatment decreased the expression of collagen I and collagen III in MRC-5 cells in a dose-dependent manner.

3.3 STS suppressed the ROS production induced by silica in MRC-5 cells.

The effect of silica is likely to be mediated by ROS, which could play an important role in the progress of pulmonary fibrosis. To determine whether STS exerts its cytoprotective effects by inhibiting ROS production, intracellular ROS levels were measured in MRC-5 stained with DCFH-DA. As shown in Fig. 4A, silica exposure could markedly increase the generation of ROS in MRC-5 cells in a dose-dependent manner. Interestingly, the macrophage/fibroblast coculture system showed a mild increase in intracellular ROS generation compared with monocultured MRC-5 cells. This finding may to some extent be due to the coexistence of the cell types and could reflect their interaction under physical conditions. On this basis, we aimed to explore

the toxic effect of silica in an *in vivo*-like system. The results showed that silica exposure could clearly aggravate intracellular oxidative stress. In consideration of this, treatment with STS markedly reduced the ROS generation induced by silica.

3.4 Effect of STS on Nrf2 protein expression in MRC-5 cells.

To investigate whether STS could affect Nrf2 expression in MRC-5 cells, the coculture system was treated with the indicated concentration of silica or STS. Following treatment for 24 h, the amount of Nrf2 protein was analyzed by Western blot and immunofluorescence in MRC-5 cells (Fig. 5). We first examined Nrf2 protein expression in whole MRC-5 cells, and the results showed that the Nrf2 expression was increased in the negative control group compared with that in the control group, whereas silica exposure caused a gradual decrease in Nrf2 expression (Fig. 5A). After STS treatment, the amount of Nrf2 protein in whole cells increased, especially at 10 μg/mL STS ($p < 0.05$) (Fig. 5B). Moreover, to further explore Nrf2 activation, the nuclear and cytoplasm levels of Nrf2 protein were determined (Fig. 5C). Silica exposure resulted in decreased levels of nuclear and cytoplasmic Nrf2 in MRC-5 cells. In addition, immunofluorescence showed that Nrf2 was barely expressed in the cytoplasm (Fig. 5D). However, the translocation of Nrf2 protein to the nucleus was significantly increased by STS treatment, as assessed using both Western blotting and immunofluorescence techniques, suggesting that STS treatment might contribute to nuclear Nrf2 protein up-regulation.

3.5 Nrf2 knockdown inhibited TrxR and Trx gene expression in MRC-5 cells.

The Trx system plays a key role in antioxidative stress. To evaluate whether the transcription factor Nrf2 could regulate the expression of TrxR and Trx, Nrf2 was knocked down by lentivirus transfection. First, shRNA-Nrf2 or shRNA-control was transfected into MRC-5 cells. After 72 h of transfection, significantly increased expression of GFP was observed in the shRNA-Nrf2 cells using an inverted fluorescence microscope (Fig. 6A). Next, Nrf2 mRNA expression was detected by RT-PCR. Compared with the shRNA-control, transfection with shRNA-Nrf2 significantly ablated Nrf2 mRNA expression at 72 h post-transfection (Fig. 6B).

These results indicate that transfection with shRNA-Nrf2 was effective in MRC-5 cells. To elucidate the downstream effectors of Nrf2, we examined Trx and TrxR mRNA expression. We found that Nrf2 knockdown by shRNA significantly decreased Trx mRNA and TrxR mRNA expression compared with the siRNA-control. This may indicate that Nrf2 was an important transcription factor that could regulate the expression of Trx and TrxR.

3.6 Effect of STS on Trx and TrxR expression in MRC-5 cells.

According to the effect of STS on the induction of Nrf2, we wondered whether the Trx system was involved in the STS mechanism of action. As shown in Fig. 6C&D, STS treatment increased Trx and TrxR protein expression, as assessed by western blotting and/or immunofluorescence analysis.

4. Discussion

Most silica particles are engulfed by macrophages in the process of entering the lung *in vivo*, and interstitial macrophages are activated after particle uptake to produce ROS (23). Therefore, this study used a macrophage/fibroblast coculture system to determine if the interaction of macrophages with silica *in vitro* could affect the underlying fibroblasts, as their activation plays a key role in the pathophysiologic process of silicosis. Fibroblasts, activated and differentiated into myofibroblasts and acquiring a pro-fibrosing phenotype, are defined by the expression of extracellular matrix proteins (collagen I and III) and cell proliferation (24). Our current study demonstrated for the first time that exposure to silica could significantly promote the proliferation and activation of MRC-5 cells in a coculture system. The results shown in Fig. 2A demonstrated that the viability of MRC-5 cells coculture with Raw 264.7 cells was increased compared with the quiescent monocultured MRC-5 cells. By contrast, macrophage/fibroblast coculture with silica treatment showed significantly increased proliferation compared with the negative control group. Additionally, collagen I and III expression was significantly increased in the silica treatment group compared with the negative control group (Fig. 3A). These results indicated that the coculture model could partially simulate the complex *in vivo* environment, enabling

the exploration of silica pathogenesis mediated by the stimulation of fibrogenesis.

The abnormal proliferation and activation of MRC-5 cells by silica could therefore be partially attributed to the increased intracellular ROS levels. First, a growing body of evidence indicates that ROS may act as a fundamental signaling molecule in many cellular processes. Previous reports have indicated that low concentrations of H_2O_2 (~10 nM–10 μM) are effective at stimulating the growth of mammalian fibroblasts in a cell culture system (25) (26). It is now clear that H_2O_2 can stimulate growth responses in a variety of mammalian cell types when added exogenously to the medium. In the present study, 10^{-5} M H_2O_2 (Fig. 2B) was needed to promote maximal proliferation of MRC-5 cells. Additionally, mice deficient for ROS production through the NADPH-oxidase pathway do not develop pulmonary fibrosis after the intranasal administration of bleomycin, suggesting that NADPH-oxidase-derived ROS are essential for the development of pulmonary fibrosis (27). These data are in agreement with previous publications indicating that there is a significant decrease in erythrocyte GSH, GPx and SOD as well as a significant increase in the MDA level in silicotic patients, suggesting oxidative stress status (28). We have previously observed that both ROS and MDA levels are markedly increased during the early stage of silica exposure in rat lung (15). Second, a recent publication also confirmed that ROS increase active TGF-β1 release, which works as a fibrotic factor and directly induces the activation of human lung fibroblasts (29). Moreover, superoxide production is markedly enhanced in vascular smooth muscle cells after TGF-β1 stimulation (30), suggesting a positive feedback loop in TGF-β1 activation by ROS. We found that the concentration of TGF-β1 in Raw 264.7 supernatants gradually increased with the silica-concentration-dependent exposure (data not shown). In this study, the results show that indirect silica exposure of fibroblasts moderately increased the generation of ROS in a dose-dependent manner and that this was accompanied by fibroblast proliferation and activation. Collectively, these data suggest that blocking fibroblast activation by scavenging excessive ROS could be a possible therapeutic approach to modulate the fibrogenic response.

Numerous reports have shown that Tanshinone IIA has antioxidant properties and

that it can alter the expression and/or activity of specific anti-oxidant enzymes to protect cells from oxidant damage (31). It has been reported that STS can markedly modulate the redox-sensitive steps to attenuate angiotensin II-induced collagen I expression in cardiac fibroblasts *in vitro* (20). In this study, we explored the potential protective mechanism of STS, which was used to treat MRC-5 cells. The results showed that both the proliferation and activation of MRC-5 fibroblasts induced by silica were reversed by STS treatment and that STS eliminated the excessive ROS production. These findings suggest that the effect elicited by STS might be due to its potent antioxidant property and its ability to mitigate fibrosis. Although the protective effects of STS against fibrosis have been widely investigated, the molecular mechanisms remain elusive, especially because the direct target of STS is unknown. The salient findings of this study are summarized as follows: 1) STS markedly decreased ROS generation via the Nrf2/Trx pathway to exert its antioxidant function; 2) STS may increase the myofibroblastic dedifferentiation associated with Nrf2 activation. These observations shed new light on the potential anti-fibrotic properties of STS in silicosis.

First, the oxidant/antioxidant imbalance in pulmonary fibroblasts was associated with decreased nuclear Nrf2 expression. Nrf2, a transcription factor, directly regulates pathways that control ROS homeostasis and antioxidant defense by modulating the transcription of critical genes to influence the onset and severity of pulmonary fibrosis. In a murine model of bleomycin-induced pulmonary fibrosis, researchers have shown increased sensitivity to bleomycin and more severe inflammatory lesions in Nrf2-knockout mice (32). In the present study, silica treatment gradually attenuated the induction of total Nrf2 in cocultured MRC-5 cells with increasing doses of silica (Fig. 5), accompanied by increasing ROS levels. Our results are in agreement with recent evidence showing decreased total Nrf2 expression in fibroblastic foci in idiopathic pulmonary fibrosis (IPF) lung biopsies (33). Moreover, the down-regulation of Nrf2 was confirmed in our previous results in a rat silicosis model, which showed that Nrf2 was absent in rat lungs on day 30 after silica inhalation (15). These results suggest that low Nrf2 expression could be the reason underlying redox

14

balance disorders. Previous studies have provided evidence indicating that the Nrf2 transcription factor binds to the ARE in the Trx and TrxR promoters in response to oxidative stress stimuli, leading to the induction of Trx and TrxR expression (34) (35) (36). We further found that Nrf2 knockdown by shRNA significantly decreased Trx mRNA expression and TrxR mRNA expression compared with the siRNA-control (Fig. 6B). Additionally, we have previously reported that silica can induce ROS accumulation and some oxidative cellular damage by down-regulating both the mRNA and protein expression of Trx and TrxR *in vitro* (37). These data are in agreement with data showing that ROS are counterbalanced by a web of antioxidant systems in the body and that the Nrf2/Trx pathway might play a key role in ROS homeostasis. However, STS treatment could significantly up-regulate the intracellular expression of Nrf2 not only in the cytoplasm but also in the nucleus (Fig. 5C&D). Furthermore, it could induce the nuclear translocation of Nrf2 and subsequently increase the protein expression of Trx and TrxR (Fig. 6C&D), which consequently enhanced the resistance to oxidative stress induced by silica. Hence, the role of STS we observed was that of facilitating Nrf2 translocation to the nucleus, where Nrf2 played a pivotal role in the transcriptional activation of Trx and TrxR, which mitigated the oxidative stress induced by silica.

Except for a clear antioxidative role in respiratory diseases, Nrf2 has been found to be involved in cellular differentiation, including the myofibroblastic differentiation of fibroblasts during IPF (38). In that study, Nrf2 knockdown induced oxidative stress and myofibroblastic differentiation in control fibroblasts. Conversely, Nrf2 activation increased antioxidant defenses and myofibroblastic dedifferentiation in IPF fibroblasts. Furthermore, Nrf2 has been found to down-regulate the collagen I mRNA level in mice (39). In agreement with this, we found that the Nrf2 down-regulation induced by silica was associated with the up-regulation of collagen I/III expression. However, STS treatment down-regulated the collagen I/III expression accompanied by Nrf2 activation. Further research is needed to explore the exact mechanism underlying the effect on STS-induced Nrf2 activation.

5. Conclusions

Our results suggest that STS likely inhibited silica-induced MRC-5 proliferation and activation by inducing Nrf2 expression and up-regulation of the oxidative response genes Trx and TrxR. This finding may form the basis of a new strategy for treating silicosis.

Conflicts of interest

The authors confirm that there are no conflicts of interest.

Fig. 1 SEM (A) and TEM (B) images of silica showing an overview of the scale structure and dispersion, with scale bars of 5 μm or 0.5 μm individually. (C) The molecular structure of STS. (D) Macrophage/fibroblast coculture system. Macrophages (Raw 264.7) were cultured on the apical side of polyester Transwell inserts (0.4 μm pore size), while lung fibroblast cells (MRC-5) were cultured in the basolateral chamber of the Transwell. Macrophages were exposed to silica particles at various doses without or with STS treatment, and the effects on the underlying fibroblasts were assayed.

Fig. 2 Effects of STS on silica/H_2O_2 induced fibroblast proliferation. Raw 264.7 and MRC-5 cells were grown in coculture, followed by exposure of different concentrations of silica/H_2O_2, as well as STS (1, 5, 10, 25, or 50 μg/mL) addition. After 24 h, cell proliferation was determined with the MTT assay. The experiments were repeated five times with reproducible results. *$P < 0.05$ vs. negative control group; #$P < 0.05$, ##$P < 0.01$ vs. the control group. & < 0.05 vs. silica/ H_2O_2 treatment group.

Fig. 3 Effects of STS on silica-induced collagen type I/III expression. Collagen type I/III expression (A&B) was determined by Western blotting. The experiments were repeated three times with reproducible results. ^$P < 0.05$ vs. control; *$P < 0.05$ vs. negative control group. #$P < 0.05$, ##$P < 0.01$ vs. silica treatment group.

Fig. 4 Effects of STS on the silica-induced production of ROS. Raw 264.7 and MRC-5 cells were grown in coculture, followed by exposure of Raw 264.7 cells to various doses of silica without or with STS (1, 5, 10, 25, or 50 μg/mL). After 24 h, DCFH-DA fluorescence was measured by a fluorospectrophotometer (A&B). The experiments were repeated three times with reproducible results. ^P <0.05, ^^P < 0.01 vs. control; *P <0.05, **P <0.01 vs. negative control group. #P <0.05, ##P <0.01 vs. silica treatment group.

Fig. 5 Effects of silica and STS on the expression of antioxidative proteins. (A&B) Western blot results are shown: one for Nrf2 in silica-treated groups (left) and one for Nrf2 in STS-treated groups (right). Silica decreased the amount of Nrf2 in whole cells, and the high dose of STS up-regulated the expression of Nrf2 in whole cells. *P < 0.05 vs. control; #P <0.05 vs. negative control group. &P <0.05 vs. silica treatment group. (C) Total form Nrf2 in the nucleus and cytoplasm were prepared and determined using Western blot. (D) Immunofluorescence staining of Nrf2 plus or minus silica and/or STS. With exposure to 50 μg/mL silica particles for 24 h, Nrf2 immunofluorescence (green) is barely observed in the cytoplasm but is clearly present with added STS. The magnification (630×) in all panels is the same. Scale bar = 25 μm. Nuclei are stained blue with DAPI.

Fig. 6 TrxR and Trx gene and protein expression in MRC-5 cells was inhibited by Nrf2 knockdown and increased by STS treatment. (A) Transfection efficiency detected by fluorescence microscopy. GFP-emitted green fluorescence (left) and same fields of vision under an optical microscope (right). More than 80% of cells were infected with lent-GFP at an MOI of 10 after 72 h of treatment. (B) Antioxidant mRNA levels by RT-PCR. The Lent-GFP-Nrf2-/- lentivirus significantly decreased the Nrf2 mRNA level and the Trx/TrxR mRNA level in MRC-5 cells. The effects of STS on Trx and TrxR protein expression, examined using immunofluorescence microscopy (C) and/or western blotting (D).

Table 1. Primer sequences.

References

1.   Cox LA, Jr. An exposure-response threshold for lung diseases and lung cancer caused by crystalline silica. Risk analysis : an official publication of the Society for Risk Analysis. 2011;31(10):1543-60.

2.   Gilberti RM, Joshi GN, Knecht DA. The phagocytosis of crystalline silica particles by macrophages. American journal of respiratory cell and molecular biology. 2008;39(5):619-27.

3.   Shen HM, Zhang Z, Zhang QF, Ong CN. Reactive oxygen species and caspase activation mediate silica-induced apoptosis in alveolar macrophages. Am J Physiol-Lung C. 2001;280(1):L10-L7.

4.   Sundaresan M, Yu ZX, Ferrans VJ, Sulciner DJ, Gutkind JS, Irani K, et al. Regulation of reactive-oxygen-species generation in fibroblasts by Rac1. The Biochemical journal. 1996;318 (Pt 2):379-82.

5.   Krieger-Brauer HI, Kather H. Antagonistic effects of different members of the fibroblast and

platelet-derived growth factor families on adipose conversion and NADPH-dependent H2O2 generation in 3T3 L1-cells. The Biochemical journal. 1995;307 (Pt 2):549-56.

6.   Lopes-Pacheco M, Ventura TG, de Oliveira HD, Moncao-Ribeiro LC, Gutfilen B, de Souza SA, et al. Infusion of bone marrow mononuclear cells reduces lung fibrosis but not inflammation in the late stages of murine silicosis. PloS one. 2014;9(10):e109982.

7.   Shi XL, Mao Y, Saffiotti U, Wang LY, Rojanasakul Y, Leonard SS, et al. Antioxidant Activity Of Tetrandrine And Its Inhibition Of Quartz-Induced Lipid-Peroxidation. J Toxicol Env Health. 1995;46(2):233-48.

8.   Shi XL, Flynn DC, Porter DW, Leonard SS, Valllyathan V, Castranova V. Efficacy of taurine based compounds as hydroxyl radical scavengers in silica induced peroxidation. Ann Clin Lab Sci. 1997;27(5):365-74.

9.   Motohashi H, Yamamoto M. Nrf2-Keap1 defines a physiologically important stress response mechanism. Trends in molecular medicine. 2004;10(11):549-57.

10.   Hawkes HJ, Karlenius TC, Tonissen KF. Regulation of the human thioredoxin gene promoter and its key substrates: a study of functional and putative regulatory elements. Biochimica et biophysica acta. 2014;1840(1):303-14.

11.   Cho HY, Jedlicka AE, Reddy SP, Kensler TW, Yamamoto M, Zhang LY, et al. Role of NRF2 in protection against hyperoxic lung injury in mice. American journal of respiratory cell and molecular biology. 2002;26(2):175-82.

12.   Papaiahgari S, Zhang Q, Kleeberger SR, Cho HY, Reddy SP. Hyperoxia stimulates an Nrf2-ARE transcriptional response via ROS-EGFR-PI3K-Akt/ERK MAP kinase signaling in pulmonary epithelial cells. Antioxidants & redox signaling. 2006;8(1-2):43-52.

13.   Kondo N, Nakamura H, Masutani H, Yodoi J. Redox regulation of human thioredoxin network. Antioxidants & redox signaling. 2006;8(9-10):1881-90.

14.   Arner ESJ, Holmgren A. Physiological functions of thioredoxin and thioredoxin reductase. Eur J Biochem. 2000;267(20):6102-9.

15.   Zhu Z, Yang G, Wang Y, Yang J, Gao A, Niu P, et al. Suppression of thioredoxin system contributes to silica-induced oxidative stress and pulmonary fibrogenesis in rats. Toxicology letters. 2013;222(3):289-94.

16.   Walters DM, Cho HY, Kleeberger SR. Oxidative stress and antioxidants in the pathogenesis of pulmonary fibrosis: a potential role for Nrf2. Antioxidants & redox signaling. 2008;10(2):321-32.

17.   Kensler TW, Wakabayashi N, Biswal S. Cell survival responses to environmental stresses via the Keap1-Nrf2-ARE pathway. Annual review of pharmacology and toxicology. 2007;47:89-116.

18.   Ma Q, He X. Molecular basis of electrophilic and oxidative defense: promises and perils of Nrf2. Pharmacological reviews. 2012;64(4):1055-81.

19.   Talalay P, Dinkova-Kostova AT, Holtzclaw WD. Importance of phase 2 gene regulation in protection against electrophile and reactive oxygen toxicity and carcinogenesis. Advances in enzyme regulation. 2003;43:121-34.

20.   Yang L, Zou XJ, Gao X, Chen H, Luo JL, Wang ZH, et al. Sodium tanshinone IIA sulfonate attenuates angiotensin II-induced collagen type I expression in cardiac fibroblasts in vitro. Experimental & molecular medicine. 2009;41(7):508-16.

21.   Kasper J, Hermanns MI, Bantz C, Maskos M, Stauber R, Pohl C, et al. Inflammatory and cytotoxic responses of an alveolar-capillary coculture model to silica nanoparticles: comparison with conventional monocultures. Particle and fibre toxicology. 2011;8(1):6.

22.   Rothen-Rutishauser B, Blank F, Muhlfeld C, Gehr P. In vitro models of the human epithelial airway barrier to study the toxic potential of particulate matter. Expert opinion on drug metabolism & toxicology. 2008;4(8):1075-89.

23.   Hamilton RF, Jr., Thakur SA, Holian A. Silica binding and toxicity in alveolar macrophages. Free radical biology & medicine. 2008;44(7):1246-58.

24.   Phan SH. Genesis of the myofibroblast in lung injury and fibrosis. Proceedings of the American Thoracic Society. 2012;9(3):148-52.

25.   Kim BY, Han MJ, Chung AS. Effects of reactive oxygen species on proliferation of Chinese hamster lung fibroblast (V79) cells. Free radical biology & medicine. 2001;30(6):686-98.

26.   Murrell GA, Francis MJ, Bromley L. Modulation of fibroblast proliferation by oxygen free radicals. The Biochemical journal. 1990;265(3):659-65.

27.   Manoury B, Nenan S, Leclerc O, Guenon I, Boichot E, Planquois JM, et al. The absence of reactive oxygen species production protects mice against bleomycin-induced pulmonary fibrosis. Respiratory research. 2005;6:11.

28.   Orman A, Kahraman A, Cakar H, Ellidokuz H, Serteser M. Plasma malondialdehyde and erythrocyte glutathione levels in workers with cement dust-exposure [corrected]. Toxicology. 2005;207(1):15-20.

29.   Qi S, den Hartog GJ, Bast A. Superoxide radicals increase transforming growth factor-beta1 and collagen release from human lung fibroblasts via cellular influx through chloride channels. Toxicology and applied pharmacology. 2009;237(1):111-8.

30.   Churchman AT, Anwar AA, Li FY, Sato H, Ishii T, Mann GE, et al. Transforming growth factor-beta1 elicits Nrf2-mediated antioxidant responses in aortic smooth muscle cells. Journal of cellular and molecular medicine. 2009;13(8B):2282-92.

31.   Li YI, Elmer G, Leboeuf RC. Tanshinone IIA reduces macrophage death induced by hydrogen peroxide by upregulating glutathione peroxidase. Life sciences. 2008;83(15-16):557-62.

32.   Cho HY, Reddy SP, Yamamoto M, Kleeberger SR. The transcription factor NRF2 protects against pulmonary fibrosis. FASEB journal : official publication of the Federation of American Societies for Experimental Biology. 2004;18(11):1258-60.

33.   Mazur W, Lindholm P, Vuorinen K, Myllarniemi M, Salmenkivi K, Kinnula VL. Cell-specific elevation of NRF2 and sulfiredoxin-1 as markers of oxidative stress in the lungs of idiopathic pulmonary fibrosis and non-specific interstitial pneumonia. Apmis. 2010;118(9):703-12.

34.   Chorley BN, Campbell MR, Wang XT, Karaca M, Sambandan D, Bangura F, et al. Identification of novel NRF2-regulated genes by ChIP-Seq: influence on retinoid X receptor alpha. Nucleic acids research. 2012;40(15):7416-29.

35.   Kim YC, Yamaguchi Y, Kondo N, Masutani H, Yodoi J. Thioredoxin-dependent redox regulation of the antioxidant responsive element (ARE) in electrophile response. Oncogene. 2003;22(12):1860-5.

36.   Sakurai A, Nishimoto M, Himeno S, Imura N, Tsujimoto M, Kunimoto M, et al. Transcriptional regulation of thioredoxin reductase 1 expression by cadmium in vascular endothelial cells: Role of NF-E2-related factor-2. J Cell Physiol. 2005;203(3):529-37.

37.   Guo W, Cao JB, Zhu ZH, Tian L. Effect of expression of TrxR and Trx on human embryo lung fibroblast cell induced by quartz. J Pract Med 2012;28:2315-7.

38.   Artaud-Macari E, Goven D, Brayer S, Hamimi A, Besnard V, Marchal-Somme J, et al. Nuclear Factor Erythroid 2-Related Factor 2 Nuclear Translocation Induces Myofibroblastic Dedifferentiation in Idiopathic Pulmonary Fibrosis. Antioxidants & redox signaling. 2013;18(1):66-79.
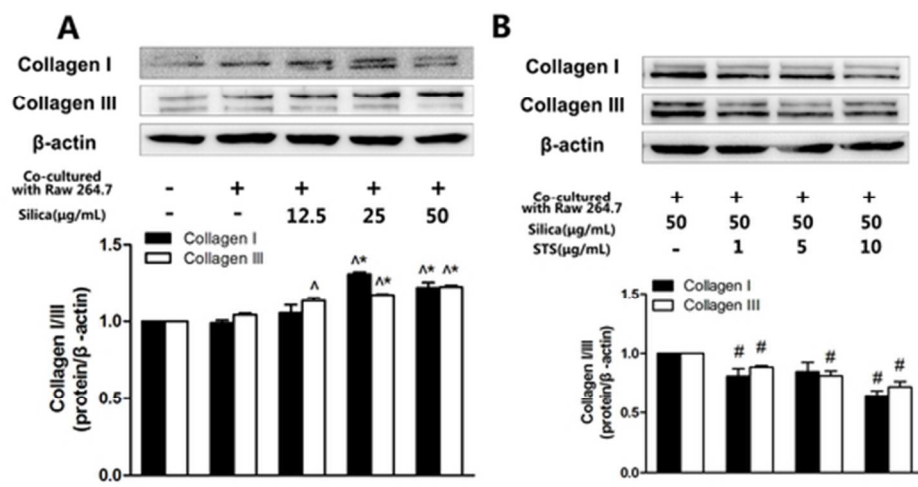
39.   Malhotra D, Portales-Casamar E, Singh A, Srivastava S, Arenillas D, Happel C, et al. Global mapping of binding sites for Nrf2 identifies novel targets in cell survival response through ChIP-Seq profiling and network analysis. Nucleic acids research. 2010;38(17):5718-34.
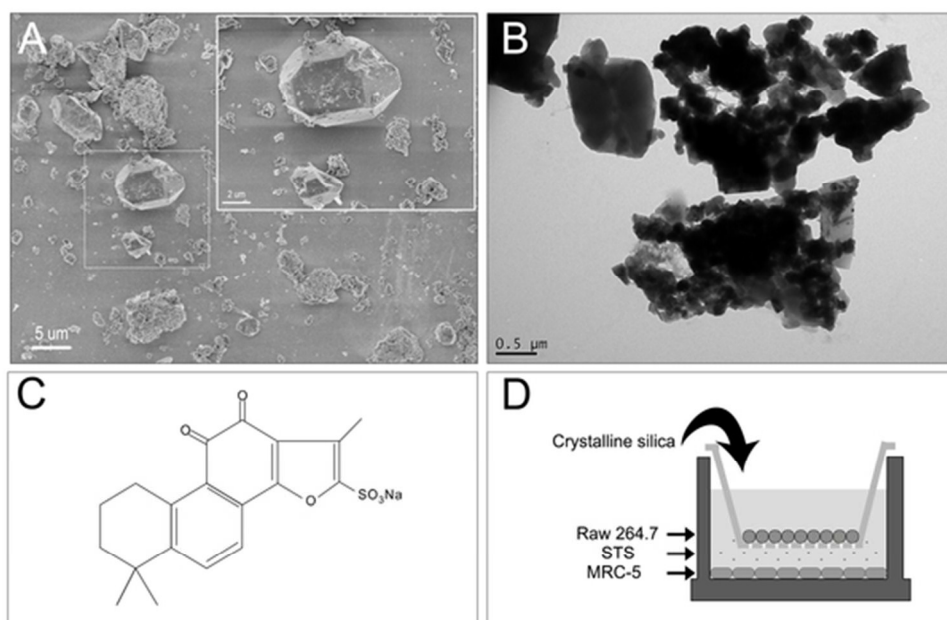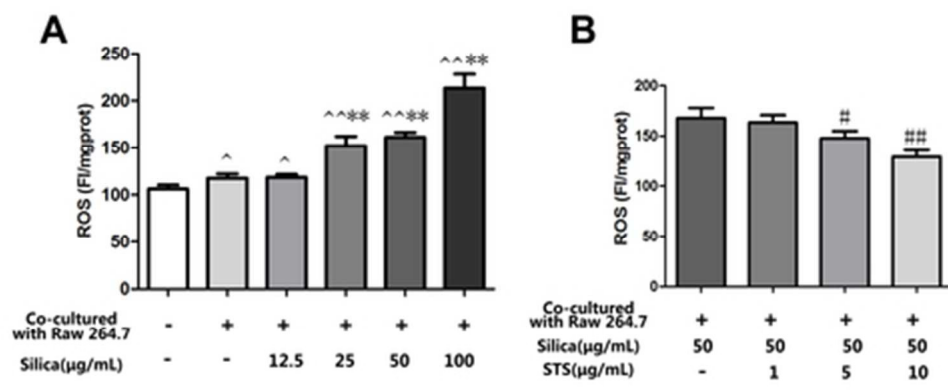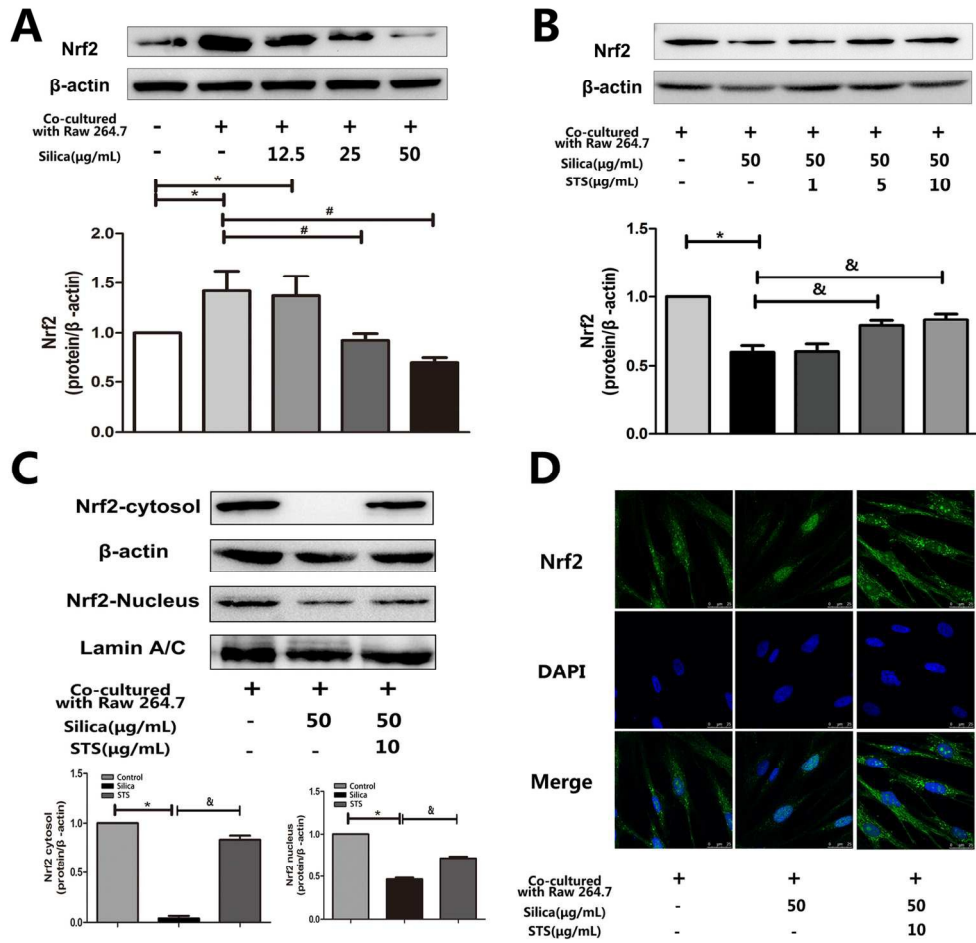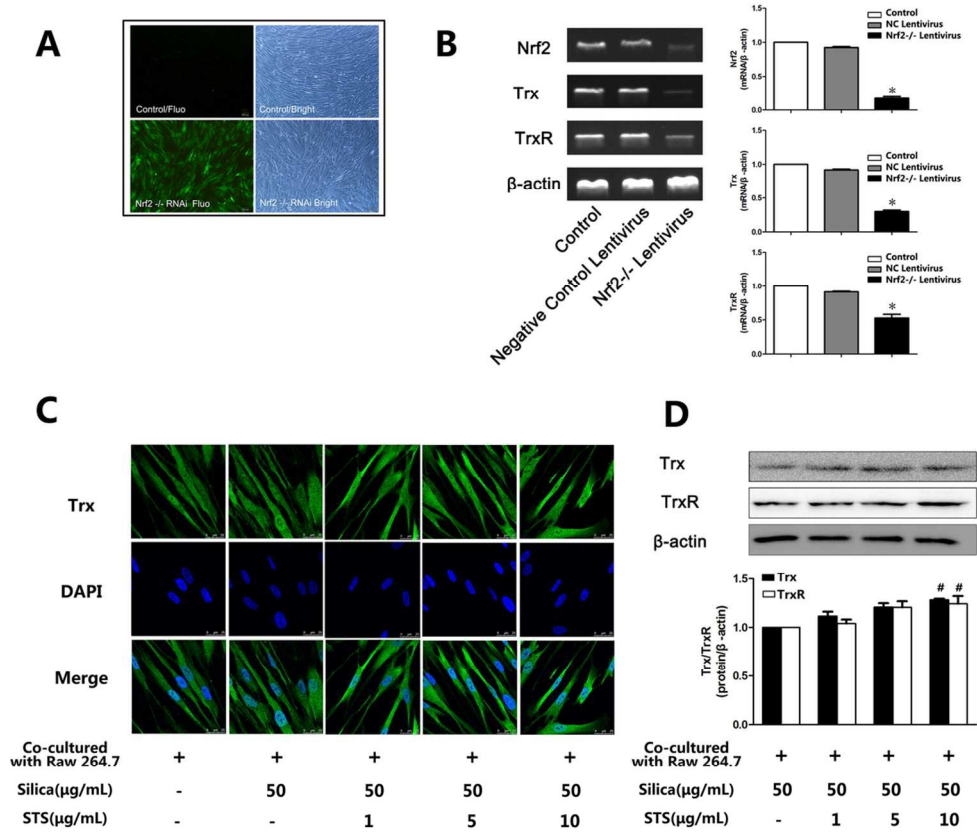
53x34mm (300 x 300 DPI)
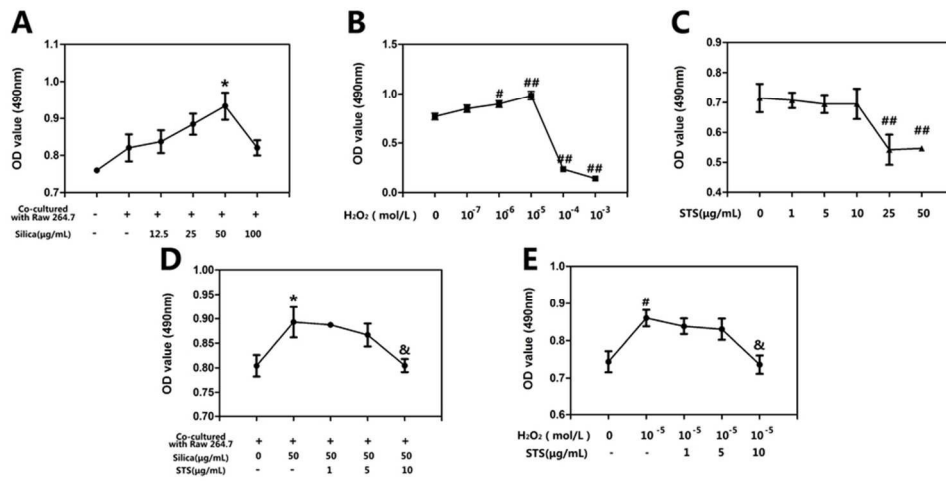
85x43mm (300 x 300 DPI)

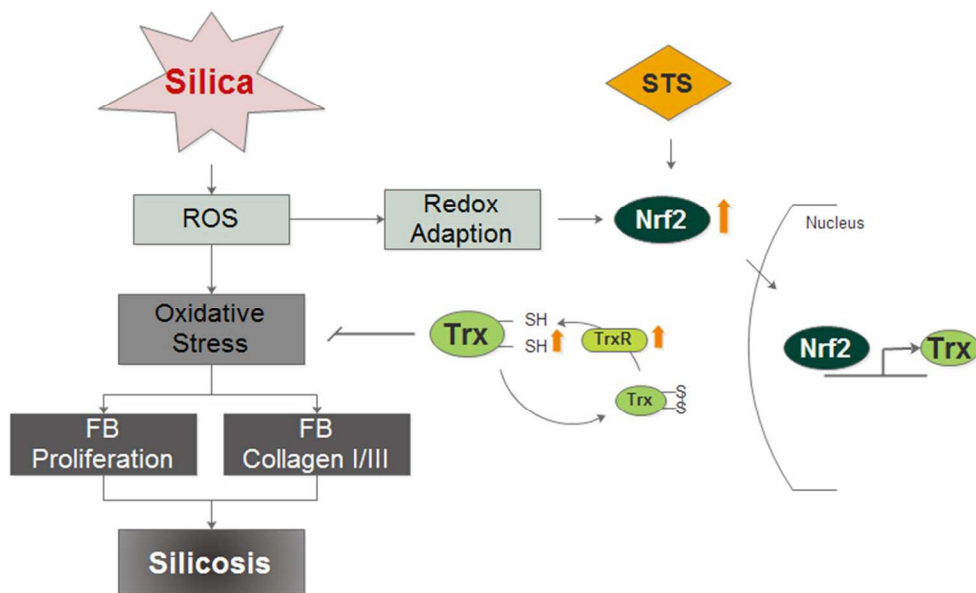50x25mm (300 x 300 DPI)

41x19mm (300 x 300 DPI)

137x134mm (300 x 300 DPI)

107x92mm (300 x 300 DPI)

β -actin,	(F) 5′ - TGAGACCTTCAACACCCCAG-3′
	(R) 5′ - GCCATCTCTTGCTCGAAGTC-3′ ;
Nrf2,	(F) 5′ - GAATTGCCTGTAAGTCCTGGTC-3′
	(R) 5′ - GGTGAAGGCTTTTGTCATTTTC-3′ ;
Trx-1,	(F) 5′ - GAAGCAGATCGAGAGCAAGACT-3′
	(R) 5′ - CACTCTGAAGCAACATCCTGAC-3′ ;
TrxR,	(F) 5′ - TCTTTTCTCCTTGCCTTACTGC-3′
	(R) 5′ - TCTTCACCCCTACGGTTTCTAA-3′ .

The graphic abstract of the role of STS.
211x128mm (96 x 96 DPI)